Organization processes of a pyropheophorbide–spermidine conjugate in the presence or absence of DNA

Souad Mansouri,[a] Suzanne Fery-Forgues,[a] Bernard Meunier[b] and Nicole Paillous*[,a]

[a] *Laboratoire des I.M.R.C.P., URA 470 au CNRS, Université Paul Sabatier, 118 route de Narbonne, 31062 Toulouse cedex, France*
[b] *Laboratoire de Chimie de Coordination, 205 route de Narbonne, 31077 Toulouse cedex, France*

The spectroscopic properties of a pyropheophorbide–spermidine conjugate, a new chemical photonuclease, are described in the absence and in the presence of DNA. The strong variations in the absorption, emission and circular dichroism spectra of this pyropheophorbide, induced by changing the solvent ethanol for phosphate buffer, indicate the occurrence of an aggregation process in aqueous solution. Addition of calf thymus (CT) DNA to a phosphate buffer solution of dye promotes biphasic variations on both the UV absorption and fluorescence spectra. These data are accounted for by an increase in the pyropheophorbide organization due to a template effect at low DNA concentrations (Dye/DNA > 1) and a redistribution of the dye on the DNA backbone at high DNA concentrations (Dye/DNA < 1). A model of the reorganization of the pyropheophorbide in the presence of DNA is proposed on the basis of a mathematical framework.

Introduction

For 10 years, there has been an explosion of activity to improve the value of photodynamic therapy (PDT) in the treatment of tumours.[1–3] A lot of new potential photosensitizers have been prepared[4–6] in order to avoid some of the disadvantages exhibited by Photofrin II, the drug currently used in PDT. Among the various classes of photosensitizers that have been established, chlorophyll derivatives appear as one of the most interesting. Pheophorbides belong to this second generation of photosensitizers which have a strong absorption in the red part of the spectrum (650–780 nm) where tissue penetration by light is extensive. Various substituted pheophorbides have recently been described.[7–12] The biological properties of these compounds (tumour cell selectivity, accumulation in tissues and side effects) vary with the nature of the macrocycle substituents, while many of the photophysical and photodynamic characteristics depend mainly on the structure of the aromatic ring and are similar to that of pheophorbide *a*. This pigment, which is among the first in this series that have been proposed for use in phototherapy,[13] displays an intense absorption at 667 nm (ε = 50 000 M^{-1} cm^{-1}), a high triplet quantum yield (Φ_{st} = 0.80) and generates singlet oxygen with a good yield (Φ = 0.51) in organic solvents such as ethanol.[14–18] In water-containing solutions, this compound has been shown to undergo an effective self-aggregation process[19] which results in a decrease in the fluorescence[20] and phosphorescence[17] lifetimes as well as in singlet oxygen formation.[17] However, the photodynamic activity of pheophorbide *a* tested in mice is greater than that of hematoporphyrin derivative (HPD) (which has a lower absorption in the visible) or of naphthocyanines (which have a lower singlet oxygen quantum yield).[21] As, in addition, this compound was shown to accumulate selectively in tumour tissues[22] it appears to be a suitable agent for cancer phototherapy and diagnosis.[21,23]

In our research for new DNA targeted photosensitizers[24–26] we have synthesized pyropheophorbide derivatives linked to polyamines.[27] The presence of a polyamine group could have two advantages: first, the occurrence of an active polyamine uptake system in many cell types,[28] and particularly in malignant cell lines, might facilitate selective accumulation of the compound in tumour tissues; secondly, the high affinity of polyamine for DNA might concentrate the cytotoxic agent near the intracellular target. The pyropheophorbide–spermidine conjugate we recently prepared, H_2PP–sp **1**, appears to be an efficient red absorbing photonuclease.[29] Upon irradiation at 690 nm, this compound induced DNA single strand break with greater efficiency than protoporphyrins excited at 400 nm.

Here, we report on the physical properties which may have an incidence on the photonuclease activity of this photosensitizer. As such compounds are known to easily undergo aggregation processes[30,31] leading to self-quenching, the organization of H_2PP–sp in aqueous buffered solutions was first investigated. In the second part, we looked for the capacity of H_2PP–sp to bind DNA. In fact, the location of this pyropheophorbide–spermidine conjugate in the cell is not known, but it has been shown that pheophorbide *a* may be rapidly incorporated into the nuclei of human cells.[32] Thus, the mode of interaction and the affinity of this compound for DNA have been determined by absorption and emission spectroscopy. The same investigations were also carried out on parent compounds bearing a shorter chain *e.g.* the pyropheophorbide-*N*,*N*,*N*-trimethylammonioethylamine conjugates, non-metallated H_2PP–TMAED **2** or zinc metallated Zn PP–TMAED **3** or deprived of a chain, *e.g.* the sodium salt of pheophorbide *a*, H_2PP–$(COONa)_2$ **4**.

Results

Spectroscopic study of pyropheophorbide derivatives in the absence of DNA

Absorption spectra. The spectroscopy of pyropheophorbides has been widely investigated in very polar organic solvents, mixtures of water and polar organic solvents and aqueous detergents where they are generally soluble.[33] It appears that their linkage to an amine chain does not affect their spectroscopic properties: the UV–VIS absorption spectrum of H_2PP–sp in ethanol (Fig. 1) displays the characteristic features of pheophytin *a*,[34,35] in particular a strong Soret band at 410 nm and a relatively strong Q_y band at 668 nm. The weak shoulder on the short wavelength side of the Q_y band has been identified as a composite of the vibrational overtones of the Q_y

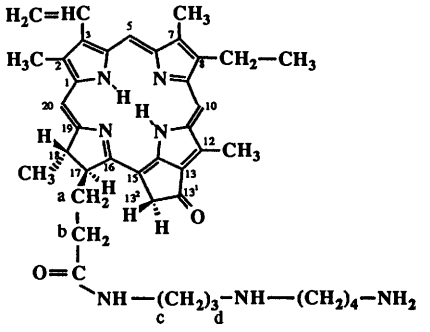

1 H_2PP–sp
pyropheophorbide–spermidine conjugate

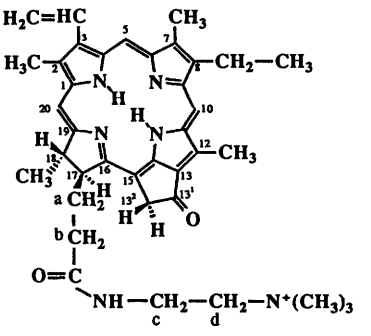

2 H_2PP–TMAED
pyropheophorbide–*N,N,N*-trimethyl ammonioethylamine conjugate

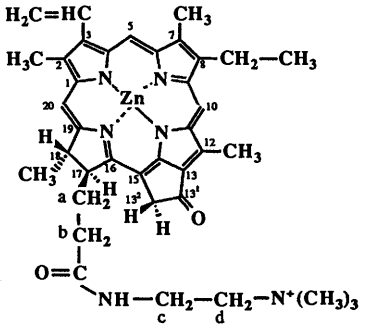

3 Zn PP–TMAED
zinc pyropheophorbide–*N,N,N*-trimethyl ammonioethylamine conjugate

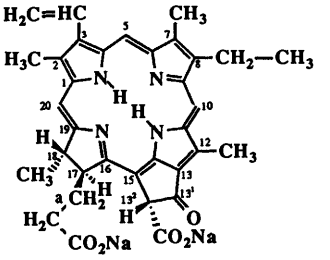

4 H_2 PP–$(COONa)_2$
sodium salt of pheophorbide a

transition.[36] The Q_x band is split (505 and 537 nm). H_2PP–TMAED and H_2PP–$(COONa)_2$ display similar spectra, and it was checked with H_2PP–$(COONa)_2$ that the position of the bands was almost unaffected by changing the organic solvent.

Unlike many natural pheophorbides, H_2PP–sp is water soluble. When passing from ethanol to phosphate buffer (pH 7.4), strong variations of its spectrum were observed (Fig. 1). The Soret band was wider, with a maximum at 388 nm and a shoulder around 442 nm. The minor intensity bands had disappeared and the Q_y band was shifted to 698 nm. Absorption intensities were greatly reduced. Molar extinction coefficients taken at the maximum of the Soret and Q_y bands were determined to be 20 000 and 10 000 M^{-1} cm^{-1}, respectively, in phosphate buffer, although they reached 48 000 and 18 000 M^{-1} cm^{-1} in ethanol. This behaviour is characteristic of aggregation in phosphate buffer, as supported by the salt effect. Addition of 200 mM NaCl to buffered solutions induced no wavelength shift of the bands, but led to an 8% hypochromic effect, indicating a reinforcement of aggregation, as the ion-solvating water became less available for dye solvation.[37] On the other hand, H_2PP–sp obeyed Beer–Lambert's law over a wide concentration range (10^{-7}–10^{-4} M). The shape of the spectrum was not affected when the temperature rose from 25 to 50 °C and the slight irreversible loss in the absorption intensity on the whole spectrum was attributed to the heat degradation of the compound. Therefore, the aggregate seems to be particularly stable.

The variations observed in the UV spectra of H_2PP–TMAED, ZnPP–TMAED and H_2PP–$(COONa)_2$ when going from ethanol to an aqueous buffered medium were qualitatively identical to those observed for H_2PP–sp. This shows that the nature of the side chain as well as the presence of a central metal atom has little influence upon the aggregation process, which appears to be an intrinsic property of the pheophorbide structure.

The spectroscopic behaviour of H_2PP–sp during the gradual

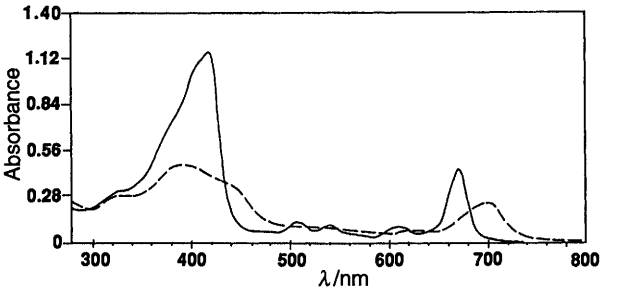

Fig. 1 Absorption spectra of H_2PP–sp (2.2×10^{-5} M) in ethanol (solid line) and in phosphate buffer (dotted line)

change of the solvent was studied in detail using binary mixtures of ethanol and phosphate buffer and a constant concentration of dye (2.3×10^{-5} M). When changing ethanol for phosphate buffer, two isosbestic points appeared at 432 and 680 nm (Fig. 2). However, the spectral variations were not monotonous: it seemed that a transitory phenomenon took place for a buffer molar fraction of around 0.27. In fact, the absorption intensity at 400 nm as well as at 668 nm decreased when the phosphate buffer molar fraction increased from 0 to 0.27, then for higher buffer contents the absorption increased again, so that the spectrum of H_2PP–sp returned to its initial value for phosphate buffer molar fractions of 0.4. This phenomenon was accompanied by the appearance of a new band centred around 708 nm. This red-shifted band exhibited a maximum intensity for a phosphate buffer molar fraction of 0.27, then decreased and disappeared for buffer molar fractions above 0.4 (see the inset of Fig. 2). The 708 nm band was formed at the expense of the 668 nm band, implying that the monomer solvated by ethanol disappeared in favour of another species. For phosphate buffer molar fractions ranging between 0.4–0.6 the spectrum of H_2PP–sp was identical to that in pure ethanol. When the phosphate buffer fraction was increased,

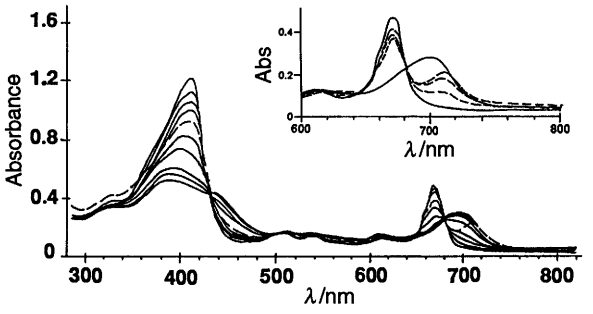

Fig. 2 Absorption spectra of H_2PP–sp (2.2×10^{-5} M) in binary ethanol–phosphate buffer mixtures. From top to bottom at 400 nm, water molar ratios: 0, 0.11, 0.13, 0.15, 0.27, 0.83, 0.89, 0.93, 0.96 and 1. Inset: evolution of the Q_y band at low phosphate buffer concentrations. From top to bottom at 668 nm, water molar ratios: 0, 0.15, 0.21, 0.27 and 1.

the absorbance decreased once more. For phosphate buffer fractions over 0.8, the 668 nm band disappeared. As the band is characteristic of the product in organic solvents, by analogy with pheophytins it may be considered to be the purest band of the monomer spectrum,[38] its disappearance indicates that no monomeric form was detected beyond a molar fraction of 0.8. This observation was confirmed by the appearance, in the same concentration range, of the 696 nm band characteristic of the aggregated form.

Fluorescence spectra. Fluorescence spectra were recorded on H_2PP–sp solutions (2.3×10^{-5} M) upon excitation at 584 nm where the absorbance was hardly modified by the aggregation process (Fig. 3). The spectrum displays only one band, with a maximum situated at 674 nm in pure ethanol and 668 nm in pure phosphate buffer. These values agree well with those given for pheophorbides.[20] In ethanol, the Stokes shift was small (6 nm) as usually observed in this series.[18] In phosphate buffer, the emission maximum (668 nm) seems to be lower than the absorption maximum (698 nm). This suggests that the emiting species was more likely to be the monomer (which was in minor proportions in the medium and should absorb at lower wavelengths) than the aggregate. The aggregate should not emit owing to self-quenching which agrees with the fact that the fluorescence intensity was 30-fold lower in phosphate buffer than in ethanol. It was reported to be 13-fold lower for pheophorbide *a* in identical conditions.[19] To support this hypothesis, 3% serum albumin was added to the phosphate buffer solution. The maximum was then at 675 nm and corresponds to a monomer in a slightly different environment. The fluorescence intensity was multiplied by a factor of at least 10, indicating that the pheophorbide was disaggregated by binding to the protein. For a phosphate buffer molar fraction of 0.21 in ethanol, *i.e.* in the concentration range where the transitory phenomenon mentioned takes place, the emission spectrum closely resembles the one obtained in pure ethanol.

Circular dichroism. The organization state of H_2PP–sp (2.3×10^{-5} M) was examined by circular dichroism. In ethanol, the CD spectrum in the Soret region was a simple positive feature, whereas it turned out to be negative in phosphate buffer. In the Q_y region, the simple negative feature observed in ethanol was converted into an eight-fold larger bisignate feature in phosphate buffer, while the wing in the Q_x region disappeared. No change was detected when going from pure ethanol to the binary mixture containing a 0.21 molar fraction phosphate buffer.

Spectroscopic study of pyropheophorbide derivatives in the presence of CT-DNA

Absorption spectra. Spectra were recorded for constant concentrations of H_2PP–sp (2.4×10^{-5} M) while the concentration of CT-DNA was allowed to vary from 5.7×10^{-6} to 2.9×10^{-4} M bp, so that the molar ratio r = [H_2PP–sp]/[DNA] varied from 4.2 to 0.08. The UV spectrum of H2PP–sp alone [Fig. 4(*a*)] changes significantly upon addition of CT-DNA. These variations can be decomposed into two steps. In a first step, as long as the molar ratio was kept above unity, the absorbance of H_2PP–sp decreased upon addition of CT-DNA. At $r = 1$, the hypochromic effect was at its maximum, the decrease in absorbance reaching 14% of the initial value for the 400 nm band [Fig. 4(*b*)]. This effect was accompanied by an 8 nm bathochromic shift of the Soret band absorption maximum, already visible in the presence of small amounts of CT-DNA. The general flattening of the Soret band may be expressed by the ratio A_{400}/A_{700} which fell from 1.9 to 1.6. It is qualitatively analogous to the one observed during aggregation.

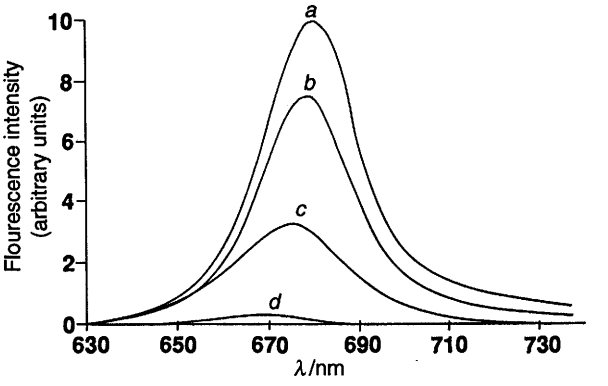

Fig. 3 Fluorescence spectra of H_2PP–sp (2.3×10^{-5} M) in ethanol (*a*), ethanol–water mixture (*b*) (water molar ratio 0.21) and phosphate buffer in the presence (*c*) and in the absence of 3% BSA (*d*). Excitation wavelength = 584 nm.

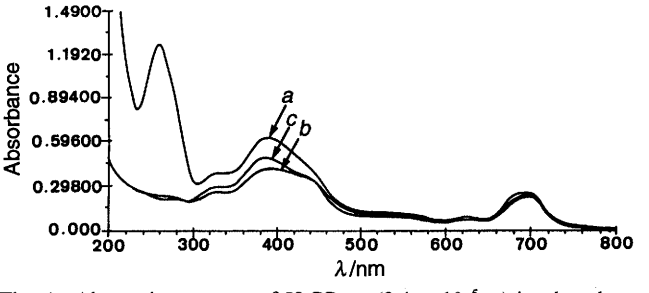

Fig. 4 Absorption spectra of H_2PP–sp (2.4×10^{-5} M) in phosphate buffer, in the absence (*a*) and in the presence of CT-DNA. DNA concentration (*b*) 1.5×10^{-7} M bp and (*c*) 2.86×10^{-4} M bp.

When increasing DNA concentrations such that r was below unity, the opposite phenomenon was observed, mainly displayed by the strong increase in absorbance over the whole spectrum. When compared with the spectra of the free dye, the spectrum of the fully complexed dye (CT-DNA > 5×10^{-4} M bp) exhibited a strong increase in absorbance of about 20% and a hypsochromic shift of 20 nm [Fig. 4(*c*)]. The ratio A_{400}/A_{700} was then 2.2, much higher than the original ratio. These variations may be visualized by plotting the absorbance recorded at 400 nm *versus* the DNA concentration (Fig. 5). A non-monotonous curve with a minimum at $r = 1$, was obtained.

Similar curves were obtained with compounds H_2PP–TMAED and ZnPP–TMAED, the absorption minima being situated at $r = 1.4$ and 4, respectively. As for H_2PP–$(COONa)_2$, the absorption spectrum was unaffected by the presence of CT-DNA in the solution.

Fluorescence spectra. In the same way, addition of increasing amounts of CT-DNA (from 1.4×10^{-6} to 2.5×10^{-4} M bp) to a solution of 6×10^{-6} M H_2PP–sp led to considerable variations in the fluorescence intensity at 670 nm (Fig. 6). Again, a two-step phenomenon took place, depending on the [H_2PP–sp]/[DNA] ratio. An almost total extinction of fluorescence was observed at low concentrations of CT-DNA, followed

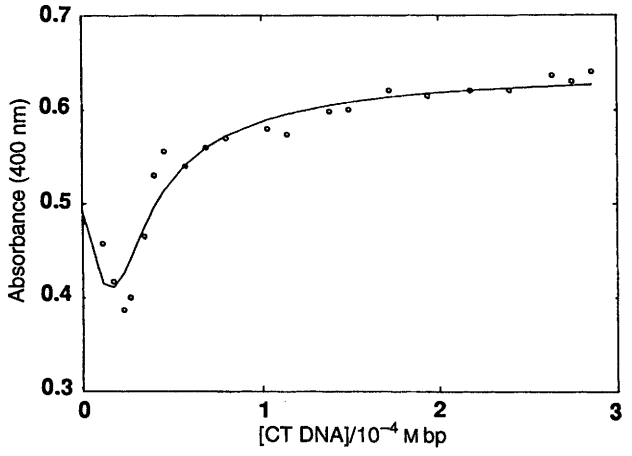

Fig. 5 Variation of the absorbance of H_2PP–sp (2.4×10^{-5} M) in phosphate buffer at 400 nm *versus* the concentration in CT-DNA. The points are experimental and the curve was calculated using Scheme 3.

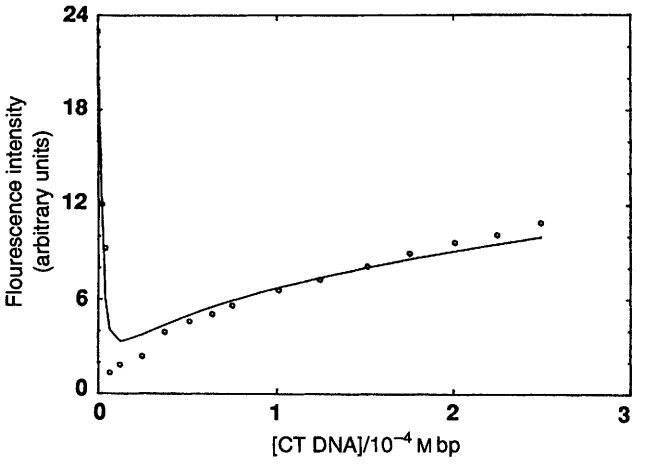

Fig. 6 Fluorescence intensity of H_2PP–sp (6×10^{-6} M) in phosphate buffer, *versus* the concentration in CT-DNA. Excitation wavelength: 380 nm. Emission wavelength: 670 nm. The points are experimental and the curve was calculated using Scheme 3.

by a partial recovery when increasing the amount of DNA. Fluorescence intensity was at its lowest for $r = 0.9$ ([DNA] = 6.9×10^{-6} M bp), this value of r being very close to the one for which minimum absorbance was observed, though the extinction of fluorescence was only partially attributable to the decrease in absorption. Similar effects were observed on the emission spectra of H_2PP–TMAED and ZnPP–TMAED, although precise determination of the minimum was made difficult by the weaker fluorescence recovery. As for absorption, the fluorescence of H_2PP–$(COONa)_2$ did not vary upon addition of CT-DNA into the solution.

Discussion

As could be expected [33] pyropheophorbide derivatives **1** to **4** are spectroscopically similar to pheophorbide *a* and pheophytine *a*, therefore confirming that the cyclic π system is the primary factor that controls the electronic properties and that the presence of ring substituents should lead to minor modifications.[39] This is in line with the similarity in spectral behaviour of the three compounds between each other and with pheophorbide *a*. In contrast, exciton interactions in chlorophyll dimer or multimeric systems were predicted to shift energies up to several hundred cm^{-1}.[36] In fact, the strong variations in the absorption and fluorescence spectra which were observed in this work, when passing from ethanol to water, are attributable to the aggregation of the pheophorbide derivatives. This is in total agreement with the fluorescence spectra and fluorescence lifetime measurements reported in the literature[20,40] which establish that pheophorbide *a* is monomeric in ethanol, but aggregated in phosphate buffer at pH 7.4.

At low water concentrations, that is for water molar ratios centred around 0.25, a transitory phenomenon takes place, mainly evidenced by the appearance of a red-shifted band at 708 nm. The transitory character of such a phenomenon may be understood in terms of water structure and by considering pheophorbides as ionic, but largely hydrophobic structures. It has been proposed[41] that in organic solvents this kind of dye could be efficiently solvated by small amounts of water. In contrast, for higher concentrations of water, the water molecules would prefer to bind to each other than to the dye ions which are therefore stabilized by ion-pairing or aggregate formation. Analogous transitory species, characterized by the red-shift of the Q_y band, have been reported by Uehara *et al.*[42] for chlorophyll *a* in THF–water mixtures. The phenomenon was at its maximum for 12% water in THF and was attributed to the formation of chlorophyll *a* dimers, bridged by two THF molecules and one water molecule. The central magnesium atom was involved in the formation of the complex, which cannot be the case here. As predicted by the calculations and stated above, the electronic structure of pheophorbide seems to be insensitive to hydrogen bonding. Again, this may be supported by the fact that a water content as high as 0.7 in molar fraction induces no shift of the maximum of the Q_y band. Thus, the shift observed during the transitory phenomenon may more likely be due to exciton interactions. On the other hand, fluorescence and CD spectra indicate that the new species must be close to the monomeric form. Therefore, it may be hypothesized that the transitory species could be a low weight cluster such as a dimer, stabilized by small amounts of water; the lack of additional information does not as yet allow a better determination of this structure.

Addition of CT-DNA to a solution of H_2PP–sp in phosphate buffer induces the appearance of a biphasic phenomenon, depending on the [H_2PP–sp]/[DNA] molar ratio. As DNA was added, the UV–VIS spectrum showed hypochromism that occurred and disappeared coincidently with fluorescence extinction. The first step may be attributed to a template-directed effect, the absorbance and fluorescence decreasing as a result of DNA-directed interactions between H_2PP–sp molecules. This is in line with the increase in organization of the product at low CT-DNA concentrations ($r > 1$) which could be attributed to the orientation of bound pheophorbide molecules on the DNA backbone, as reported for porphyrins.[43,44] Higher CT-DNA concentrations seem to induce a statistical redistribution of H_2PP–sp along the DNA strands. Comparison of the spectra of H_2PP–sp alone in phosphate buffer and those of H_2PP–sp in the presence of saturating amounts of CT-DNA indicates that destacking has occurred in the presence of DNA, although the spectral characteristics of the bound pheophorbide molecule remain far from those of the monomeric form in ethanol.

In the literature, an analogous variation of the UV–VIS spectra was encountered during the binding of ruthenium salts to DNA.[45] Similar behaviour displayed by the UV and fluorescence spectra has also been reported to take place during the binding of anthrylpolyamines to biological polyanions such as heparin and poly-L-glutamate.[46,47] The biphasic phenomenon was attributed to template-directed excimer formation taking place at high molar ratios and followed by redistribution of the fluorophore over the length of the polyanion when the polyanion concentration was increased.

In our work, two different hypotheses may be proposed to account for the observations: either the monomer present in the solution only or the aggregated form may bind to CT-DNA. Two biphasic mechanisms can then be written. The first hypothesis considers that the pyropheophorbide monomer P is the only form able to bind to DNA and that this binding displaces the first equilibrium and leads to the disappearance of

the aggregated form (Scheme 2). For the sake of simplicity, the

$$P_2 \underset{k_2}{\overset{k_1}{\rightleftharpoons}} 2P$$

$$P + DNA \underset{k_4}{\overset{k_3}{\rightleftharpoons}} DNA\text{–}P$$

Scheme 2

aggregated form has been written as a dimer P_2. The second possibility is given in Scheme 3. In this case, the aggregate binds

$$P_2 + DNA \underset{k_2}{\overset{k_1}{\rightleftharpoons}} 2\,DNA\text{–}P_2$$

$$DNA\text{–}P_2 + DNA \underset{k_4}{\overset{k_3}{\rightleftharpoons}} 2\,DNA\text{–}P$$

Scheme 3

to DNA and is then redistributed along the strands when the concentration of DNA increases.

Modelling was carried out in order to test the two hypotheses according to the absorption and fluorescence data. The two models yield differential equations which express the evolution of the chemical species. The differential equations were integrated numerically until the equilibrium state was reached. The values of the parameters k_1, k_2, k_3 and k_4 were refined using a non-linear minimization algorithm of the Powell type in order to improve the fit between the model and experimental data. The first model does not fit the experimental points and can be ruled out. The second one provides an interesting fit of both UV and fluorescence curves (Figs. 5 and 6) and so deserves to be considered. It must be emphasized that this model is very simplified, the aggregate being written as a dimer. Besides, errors may have been introduced in the estimation of the spectral parameters of the bound dye. It should be observed that adding another equilibrium $P_2 \rightleftharpoons 2P$ to the second model does not improve the fit. Absorption and fluorescence data provided similar equilibrium constants K_1. ($K_1 = k_1/k_2 = 2.1 \times 10^6$ and 1.8×10^6, respectively). In contrast, the equilibrium constant $K_2 = k_3/k_4$ was far higher when calculated from absorption (5.7) than from fluorescence data (6×10^{-3}). These values must be taken just as estimates and in no way can be compared with those determined for other products by the McGhee–von Hippel method, classically used to calculate the binding constants of dyes with DNA and which cannot reasonably be applied here. Anyway, it is likely that the binding constant of the first step, which corresponds to external binding to a polyelectrolyte is far higher than the binding constant of the second step. Further experiments are in progress in order to determine the binding mode of the redistributed monomer.

Modelling was not undertaken for the other pheophorbide derivatives. However, taking into account the similarities in behaviour for close ranges of concentrations, it seems that little difference can be found in the affinity of products **1**, **2** and **3** towards DNA, showing that substitution by a spermidine chain, as well as metallation, does not lead to any major improvement of the binding. As for the $H_2PP(COONa)_2$ derivative, the negative charge borne by the molecule prevents any interaction with DNA from being established.

Experimental

Materials

The details of the methods of preparation and purification of pyropheophorbide *a* derivatives have been given previously.[28,30] Calf thymus (CT) DNA (highly polymerized sodium salt, form I) was purchased from Sigma Chemical Co. and used without further purification. Solutions were prepared in absolute ethanol (Prolabo) or phosphate buffer pH 7.4 (5 mM KH_2PO_4, 5 mM $Na_2HPO_4{\cdot}H_2O$, 10 mM NaCl, in twice distilled water).

Apparatus and methods

Absorption spectra were recorded at 25 °C using a Hewlett-Packard 8452A diode array spectrophotometer. Corrected emission spectra at 25 °C were obtained on an AMINCO SPF 500 spectrofluorimeter. The absorbance of the sample was below 0.07. The bandwidth was 2 nm for both emission and excitation. Dichroism spectra were carried out on a Jobin Yvon MARK V dichograph, interfaced with an Apple II GS microcomputer for storage and analysis of the data. Calculations were performed on an HP 9000 series 710 work station running under UNIX with a program previously developed in our laboratory to analyse photochemical equilibria provided the mathematical framework for modelling.

Acknowledgements

Thanks are expressed to Professor J. Sotiropoulos for his kind help in circular dichroism measurements and to Mr D. Lavabre for his assistance in the calculations.

References

1 T. J. Dougherty, *Photochem. Photobiol.*, 1989, **45**, 879.
2 D. Kessel, *Photodynamic Therapy of Neoplastic Disease*, CRC Press, Boca Raton, 1990, vol. 2.
3 S. L. Marcus in *Photodynamic Therapy, Basic Principles and Clinical Applications*, eds. B. W. Hendersen and T. J. Dougherty, Marcel Dekker, New York, 1992, pp. 219–268.
4 T. J. Dougherty, *Photochem. Photobiol.*, 1987, **45**, 879.
5 G. Bock and S. Harnett, *Photosensitising Compounds: their Chemistry, Biology and Clinical Use*, Ciba Foundation Symposium 146, Wiley, Chichester, 1989.
6 R. Bonnett, *Chem. Soc. Rev.*, 1995, **24**, 19.
7 R. K. Pandey, D. A. Bellnier, K. M. Smith and T. J. Dougherty, *Photochem. Photobiol.*, 1991, **53**, 65.
8 R. K. Pandey, F. Y. Shiau, A. B. Sumlin, T. J. Dougherty and K. M. Smith, *Bioorg. Med. Chem. Lett.*, 1992, **2**, 491.
9 D. A. Bellnier, B. W. Henderson, R. K. Pandey, W. R. Potter and T. J. Dougherty, *J. Photochem. Photobiol., B*, 1993, **20**, 55.
10 T. Ando, Y. Suzuki, R. Geka, K. Irie, K. Koshimizu, T. Takemura, S. Nakajima and I. Sakata, *Tetrahedron Lett.*, 1991, **32**, 5107.
11 S. Gatt, A. Dagan, R. Santus, J.-C. Maziere, J. D. Chapman and E. L. Engelhardt, *PCT. Int. Appl.*, 1995.
12 M. Karasawa, T. Otani, M. Uchimoto, K. Aizawa and H. Kawabe, EP 322 198/1989.
13 B. Roeder, *Stud. Biophys.*, 1986, **114**, 183.
14 A. A. Krasnovsky, Jr., *Photochem. Photobiol.*, 1979, **29**, 29.
15 S. Kimura, *Photomed. Photobiol.*, 1987, **9**, 35.
16 S. Yu. Egorov, A. A. Krasnovski and B. Roeder, *Opt. Spektrosk.*, 1988, **64**, 790.
17 A. A. Krasnovsky, Jr., K. V. Neverov, S. Yu. Egorov, B. Roeder and T. Levald, *J. Photochem. Photobiol., B.*, 1990, **3**, 245.
18 B. Roeder, D. Naether, T. Lewald, M. Braune, C. Nowak and W. Freyer, *Biophys. Chem.*, 1990, **35**, 303.
19 I. Marlow, F. Marlow, B. Roeder and H. Stiel, *Z. Chem.*, 1986, **26**, 338.
20 B. Roeder and H. Wabnitz, *J. Photochem. Photobiol., B*, 1987, **1**, 103.
21 B. Roeder, *J. Photochem. Photobiol. B*, 1990, **5**, 519.
22 N. Maeda, K. Ichikawa, I. Kobayashi and N. Mizuno, *Clin. Res.*, 1985, **33**, A663.
23 S. Kimura, *Photomed. Photobiol.*, 1993, **15**, 1.
24 C. Sentagne, B. Meunier and N. Paillous, *J. Photochem. Photobiol., B*, 1992, **16**, 47.
25 C. Sentagne, S. Fery-Forgues, B. Meunier and N. Paillous, *New J. Chem.*, 1994, 18, 1253.
26 C. Sentagne, J.-C. Chambron, J.-P. Sauvage and N. Paillous, *J. Photochem. Photobiol., B*, 1994, **26**, 165.

27 S. Mansouri, B. Meunier, A. Gossauer and N. Paillous, *New J. Chem.*, 1994, **18**, 74.
28 N. Seiler and F. Dezeure, *Int. J. Biochem.*, 1990, **22**, 211.
29 S. Mansouri, B. Meunier, A. Gossauer and N. Paillous, unpublished results.
30 G. L. Closs, J. J. Katz, F. C. Pennington, M. R. Thomas and H. H. Strain, *J. Am. Chem. Soc.*, 1967, **89**, 4703.
31 L. J. Boucher and J. J. Katz, *J. Am. Chem. Soc.*, 1963, **23**, 3809.
32 M. Kobayashi, S. Koyama, K. Isaka, H. Harada, N. Miyoshi, C. Wolff, C. Tanielan, M. Sasaki and M. Komiyama, *Photomed. Photobiol.*, 1993, **15**, 75.
33 J. D. Spikes and J. C. Bommer, in *Chlorophylls*, ed. H. Sheer, CRC Press, Boca Raton, 1991, pp. 1186–1187.
34 J. C. Goedheer, in *The chlorophylls*, eds. L. P. Vernon and G. R. Seely, 1960, ch. 6.
35 H. K. Lichtenthaler, *Methods Enzymol.*, 1987, **148**, 350.
36 A. J. Hoff and J. Amesz, in *Chlorophylls*, ed. H. Sheer, CRC Press, Boca Raton, 1991.
37 R. B. McKay and P. J. Hillson, *Trans. Faraday Soc.*, 1965, **61**, 1800.
38 M. Van Gurp, G. Van Ginkel and Y. K. Levine, *Biochem. Biophys. Acta*, 1989, **973**, 405.
39 L. K. Hanson, in *Chlorophylls*, ed. H. Sheer, CRC Press, Boca Raton, 1991, pp. 724–726.
40 F. Adam, B. Röder, H. Stiel and H. Wabnitz, *Teubner-Texte Phys.*, 1987, **13**, 221.
41 M. J. Blandamer, M. C. R. Symons and G. S. P. Verma, *J. Chem. Soc., Chem. Commun.*, 1965, 629.
42 K. Uehara, Y. Hioki and M. Mimuro, *Photochem. Photobiol.*, 1993, **58**, pp. 127–132.
43 R. F. Pasternack and A. Giannetto, *J. Am. Chem. Soc.*, 1991, **113**, 7799.
44 R. Kuroda and H. Tanaka, *J. Chem. Soc., Chem. Commun.*, 1994, 1575.
45 C. Hiort, P. Lincoln and B. Nordén, *J. Am. Chem. Soc.*, 1993, **115**, 3448.
46 S. A. Van Arman and A. W. Czarnik, *J. Am. Chem. Soc.*, 1990, **112**, 5376.
47 C. V. Kumar and A. Chandhari, *J. Am. Chem. Soc.*, 1993, **115**, 8457.

Paper 6/00684A
Received 30*th January* 1996
Accepted 17*th April* 1996